AN ELECTROTHERMALLY-DRIVEN LOW VOLTAGE MICRO SWITCH FOR HIGH FREQUENCY APPLICATIONS

P. MAHMOUDI
Department of Electrical Engineering, Payame Noor University
PO BOX 19395-3697 Tehran, IR of Iran, parisamahmoudi2@gmail.com

A. MAHMOUDI
Department of Computer and Electrical Engineering, University of Tabriz, Iran
venchenzo06@yahoo.com

Abstract: In this paper, a MEMS switch with single layer arms has been designed and demonstrated. The switch has been actuated by combination of electrostatic and thermal actuation methods. Most of common thermal switches have been fabricated on several layers. But this will be result in difficult and high cost fabrication processes. Avoiding these problems, the shunt MEMS switch has been proposed. It can greatly simplify the fabrication process and reduce cost. High frequency simulation results show that the insertion loss is lower than 0.5 dB and the isolation is -40 dB at 2 GHz. By the combination actuated way, the electrostatic actuation voltage is reduced to 5v. So the switch can be integrated with standard CMOS circuits without any up-converters. The switching time is about 70μs and the maximal temperature of thermal actuator is lower than 150° C which cannot cause any longtime damage.

Key words: RF MEMS, termoelectrostatic actuation, pull in voltage, isolation, insertion loss.

1. Introduction.

So-called MEMS (micro-electromechanical systems) are now the subject of a vast amount of scientific and technological works [1-2]. MEMS are currently predicted to lead to a second silicon technological revolution. MEMS are devices made by the integration of mechanical structures and multifunctional materials alongside microcircuits all on one and the same chip.

Actuators, sensors, micro-pumps, micro-switches, micro-motors and other micrometer-sized devices are being monolithically integrated with transistors to create new generations of micro-systems.

The MEMS-based switches are basic building blocks in satellite, radar and wireless communication systems. RF MEMS switches offer superior RF characteristics as compared to other electronic and mechanical switches. While mechanical switches have good RF characteristics, they are heavy and costly. Electronic switches are light but give poor RF characteristic and nonlinearity and consume more power. The RF MEMS switches combine the advantages of both mechanical switches and electronic switches. They can be primarily classified as capacitive (shunt) or metal-to-metal contact (series) types [3-6]. The

MEMS switch utilizes several different actuation mechanisms including electrostatic, thermal, magnetic, and piezoelectric [7-8].

Electrostatic actuation has been the focus of a majority of the MEMS switch designs.

However, reliability concerns and reduction of high pull-in voltage are its important challenges [9-10]. Usage of combination of actuation methods has had a good effect on pull in reduction [8].

On the other hand, most of common combined thermo-electrostatic actuated switches have had a similar multi-layer complicated fabrication process [11-12]. But this work proposes a different process which is easier and simpler.

In the first section of this paper the switching behavior of an electrostatic actuated switch has been studied by a one-dimensional analytical method. The pull-in and release voltages have been described too. In the next section the combined thermoelectrostatic actuated shunt switch has been proposed and its complete dynamic operation explained. All its functional properties have been simulated through 3D finite element methods, and then high frequency parameters of the switch extracted. At the end, the fabrication process of the switch has been proposed.

2. Electrostatic actuation and pull in

Fig. 1 shows an electrostatically actuated fixed-fixed micro-switch. The device consists of a beam. It is suspended over a dielectric film deposited on top of the center conductor and fixed from both ends to the ground conductor.

When a voltage is applied between the upper and lower electrodes, the upper deformable beam is pulled down due to the generated electrical force.

The microstructure balance is dependent to electrostatic attractive force and mechanical (elastic) restoring force which are increased when the electrostatic voltage increases.

When the voltage reaches the critical value, pull-in instability occurs at which the elastic restoring force
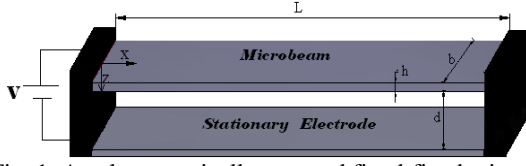
Fig. 1. An electrostatically actuated fixed-fixed micro-beam [13].

Fig. 2. Lumped model, F_e and F_t are the electrostatic actuating and elastic restoring forces respectively [14].

can no longer balance the electrostatic force. Further increase of the voltage leads to pull down the structure.

The governing equation for the static deflection of the Euler-Bernoulli beam $w(x)$ actuated by an electrostatic load of voltage V is written as Eq. (1).

$$EI \frac{\partial^4 w}{\partial x^4} = \frac{\varepsilon_0 b}{2} \left(\frac{V}{d - w(x)} \right)^2 \qquad (1)$$

where E is the Young's modulus. $I = bh^3/12$ is the effective moment of inertia of the cross-section which is relative to thickness and width, ε_0 and d are the dielectric constant of the gap medium and initial gap, respectively.

Due to the nonlinearity of the static equation, the solution is complicated and time consuming. Direct applying of Galerkin method or finite difference method creates a set of nonlinear algebraic equation. This equation can be solved by Galerkin based SSLM method [13]. On the other hand for convenience in the analysis, a one-degree of freedom lumped model can be used. A lumped model can be helpful to gain a rough quantitative estimation for the response of a wide range of electrostatically actuated microstructures [14-15]. The lumped model shown in Fig. 2 is utilized to represent a MEMS switch with electrostatic actuation.

The device has a movable microstructure which forms one side of a parallel-plate capacitor. A spring of coefficient k_m is used to model the effective stiffness of the microstructure, which is due to the elastic restoring force. The plates are distanced by a gap x_0 according to Fig. 2. This one dimensional model uses a single spring constant for the entire device behavior and the plates overlapping area of A. All fringing effects in the electrostatic analysis and the distributed capacitance of the deformed plates are neglected [16-17]. There is a rigid stop at a distance x_d above the ground plane which corresponds to an insulating layer on the ground electrode in actual devices and ensures that the two electrodes not to come into contact.
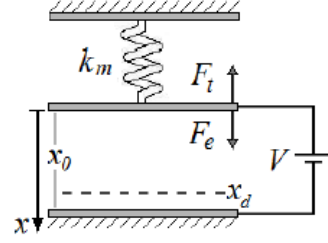
The force balance equation for this model can be written as Eq. (2) by summing together the actuating nonlinear electrostatic force, Fe and the linear restoring force due to the spring, Ft.

Static equilibrium occurs where the electrostatic force lines and the mechanical force line cross each other. Damping force is neglected for the static equilibrium [16, 18].

$$0 = F_t + F_e = -k_m x + \frac{\varepsilon_0 A}{2(x_0 - x)^2} V^2 \qquad (2)$$

where x determines displacement. At the pull-in point, both the electrostatic and mechanical forces are equal in magnitude and slope. So pull-in voltage can be calculated as Eq. (3),

$$V_{pl} = \sqrt{\frac{8 k_m x_0^3}{27 \varepsilon_0 A}} \qquad (3)$$

Stable static solutions occur before the pull-in point, while unstable (dynamic) solutions occur after. The maximum stable position for parallel plate actuator occurs at one-third the gap between the electrodes. This is shown for proposed micro switch once it is actuated electrostatically in Fig. 3.

The pulled in plate can be kept down by a voltage lower than pull-in voltage, which called release voltage. It can be calculated in the same way as Eq. (4),

$$V_{re} = \sqrt{\frac{k_m x_d (x_0 - x_d)^2}{\varepsilon_0 A}} \qquad (4)$$

Pull in and release voltages are 10.5v and 3.3v from calculation respectively.

3. Design and operation

The schematic diagram of the shunt MEMS switch is shown in Fig. 4. Symmetry of the plan makes its analysis simpler and faster, so that one fourth of the switch can be analyzed.
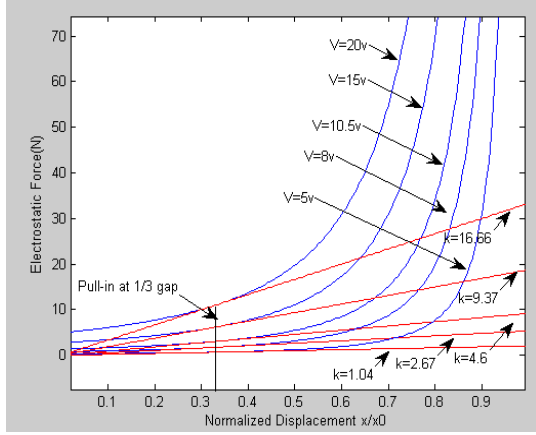
Fig. 3. Intersection points of electrostatic and restoring forces, showing pull in, stable and unstable positions.
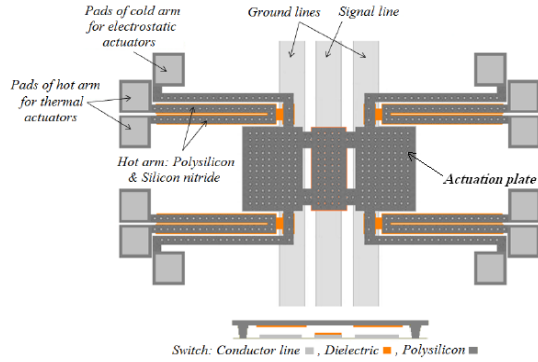

Fig. 4. Schematic of the switch.

The mechanical design of the 1/4 of the switch consists of folded suspensions of serpentine format. These springs have been attached to a square plate which electrostatically actuates the switch. The center plate attached to the actuation plate provides a parallel capacitance at the center conductor of the finite ground coplanar waveguide (FGCPW) line below the switch and creates the switch up and down states.

The entire structure is anchored to the substrate at the ends of the folded suspensions using pads as shown in Fig. 4.

The actuation plate is the electrostatic part of actuation and voltage is applied to it using transducer elements of finite element analysis (Fig. 5). The transducer element converts energy from the electrostatic domain into the mechanical domain and results in the switch motion. It represents the capacitive response of a device to motion in one direction and is used to simulate electrostatic and mechanical coupling of the structure. For the presented switch, electrostatic field is simulated using transducers underneath the actuation plate.
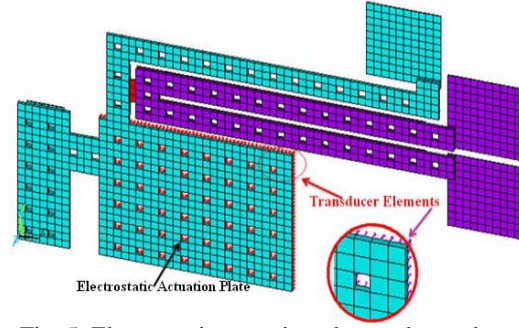

Fig. 5. Electrostatic actuation plate and transducer elements.

The applied voltage is lower than the calculated pull-in voltage for the switch but is higher than its release voltage. Also hot arms are the thermal part of actuation. Voltage is simultaneously applied to the pads of hot arms and actuation plate. So the switch is pulled in. Once the switch clamps down, the high capacitance present at the center conductor provides a virtual short at RF. The contact time is at 45 µs (Fig. 6).

After contact creation, the applied voltage is only eliminated from hot arms pads. This cut off way decreases power dissipation in comparison with just thermal actuation mechanisms.

Usage of thermal actuation, in such a short time, keeps the dissipation energy of switch lower than any critical range in comparison with merely thermal switches.

Thereafter, the switch can remain in the off (down) state until a desired time using the electric field created by Transducers (till 200µs as shown in Fig. 6 for the proposed switch). Elimination of transducers voltage will remove the contact immediately.

After elimination of applied voltage from electrostatic actuator, the switch moves immediately up and makes the transmission line connect, as shown in Fig. 6. It will be possible if the hot arms have enough time to cool down. The reverse process needs about 20µs to remove the coupling between the contact plate of the switch and the center plate of the FGCPW line from the diagram.

In this design, the supply voltage for electrostatic actuator is 5 volt, which is light over the switch release voltage. This voltage is lower than the electrostatic pull-in voltage, so the switch can work easily without the need for any CMOS up-converters. The simulation results showed that the same voltage quantity is adequate for thermal pads, too.

4. RF parameters

The performance of RF MEMS switches is determined on the base of their operational parameters called isolation and insertion loss.

The insertion loss of an RF device is a measure of its efficiency for signal transmission. In the case of a switch, the insertion loss is specified only when its state is such that signal is transmitting or when the switch is in the on-state. This is specified in terms of the transmission coefficient, in decibels, between the input and output terminals of the switched circuit. Usually specified in decibels, one of the design goals for most of the RF switches is to minimize the insertion loss. RF MEMS switches can be designed to operate with a small insertion loss at several Giga Hertzes.

The isolation of a switching system is specified when there is no signal transmission. This is measured between the input and output terminals of the switched circuit, under the no-transmission state or when the switch is in the off condition. A large value (in decibels) indicates very small coupling between input and output terminals. Thus the design goal is to maximize the isolation. In RF MEMS switches isolation may degrade as a result of proximity coupling between the moving part and the stationary transmission line as a result of leakage currents.

The simulation results for the insertion loss and isolation are shown in Fig. 7. The insertion loss is 0.48 and 1.03 dB at 2 and 4 GHz, with isolation of 43 and 38 dB, respectively.
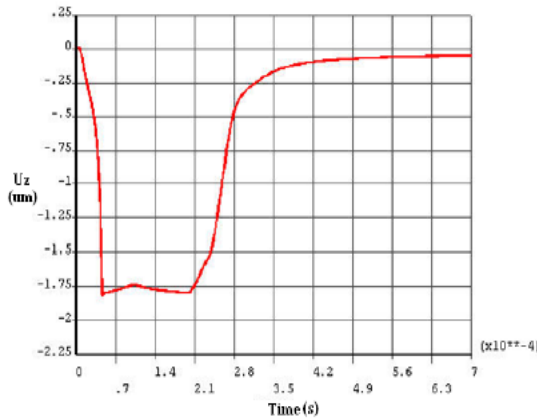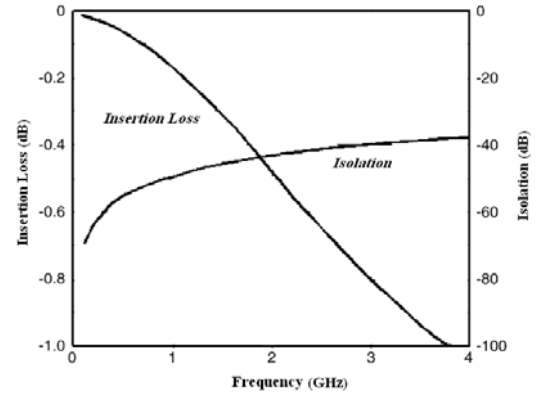

Fig. 6. Displacement curve of contact plate.

Fig. 7. RF characteristics simulation results.

5. Fabrication

Polysilicon is the main material of the switch. The switch thermal actuator consists of a cold and two hot polysilicon arms which are structured on the same polysilicon layer. Only one additional layer of silicon nitride is used to connect both hot and cold arms. The silicon nitride is deposited under hot polysilicon arms, which makes a thermal material bimorph system [19] (Fig. 8). That guaranties a down deformation of the thermal actuator due to lower coefficient of thermal expansion of silicon nitride in comparison with polysilicon.

All of the arms of the proposed switch were formed in the same surface and motion in the desired direction was guaranteed with respect to a bi-material additional system which was explained. This could not damage the switch because its temperature didn't increase so much and the silicon substrate underneath the arms wasn't destroyed (Fig. 9). In this design the transmission line width is selected smaller than the contact plate once. Using this way, forces used to the contact area will be decreased. So the mechanical stiction occurring probability will be decreased too.
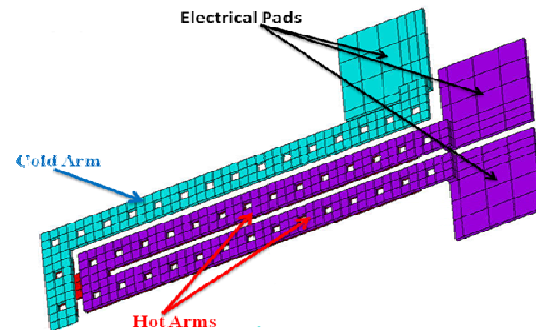

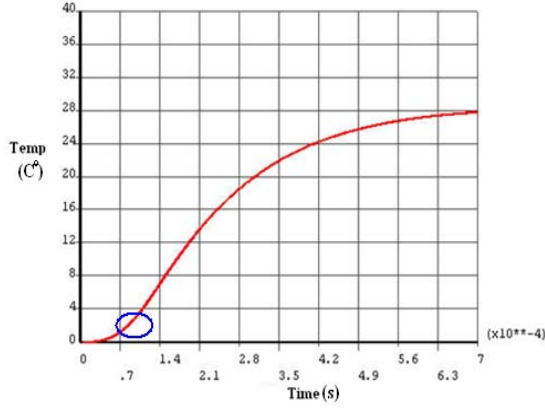Fig. 8. Main parts of the proposed thermo electrostatic actuator.

Fig. 9. The curve of temperature distribution on the contact plate.

The Holes is originally used to etch the sacrificial layer underneath the structure by fabrication. Using holes in the contact plate of the structure increases the switch isolation by decreasing coupling between CPW line and the plate below. In the case of the actuation plate, holes existence can decrease perimeter damping effect and so increase switching speed. Also holes decrease spring stiffness of the structure. So it is expected lower pull in voltage for the switch. Large area selection for the actuation plate is done for the same aim [20]. Surface micromachining technique is used for the fabrication process. The proposed process is completely compatible to MMIC fabrication technology and is the easiest and lowest cost one with respect to the same material existence for the substrates.

According to Fig. 10, the surface of silicon wafer is covered with a thin silicon nitride layer. Then CPW lines are patterned on the silicon substrate using lift off process and gold evaporation.

At the next stage, 0.5µm silicon nitride is deposited and patterned on the central conductor of the CPW line to configure the shunt switch (Fig. 11). To form the main structure of the switch, 2µm silicon oxide layer is deposited as a sacrificial layer and then patterned using photolithography.

Then marked places on it are eliminated using etching for silicon nitride deposition as shown in Fig.12. The width of the sacrificial layer determines the air gap between switching electrode and CPW line. Then the sacrificial layer is etched again to form the anchors (Fig. 13). Then, according to Fig. 14, 2µm polysilicon layer is deposited as the switch main material. At the end, the sacrificial layer is eliminated using HF acid to complete the fabrication process (Fig. 15).

Fig.10. Formation of CPW line on the substrate, using lift off.
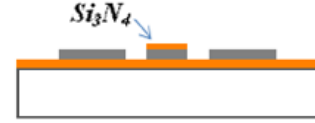

Fig. 11. Deposition and patterning of silicon nitride on the central conductor line.
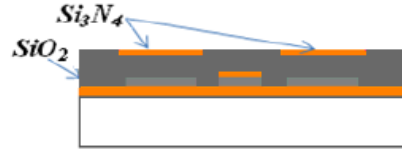

Fig. 12. Deposition of Silicon oxide and then silicon nitride.

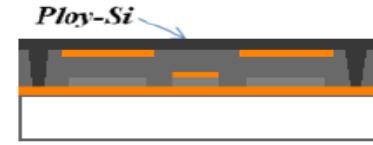Fig. 13. Etching of sacrificial layer to form anchors.
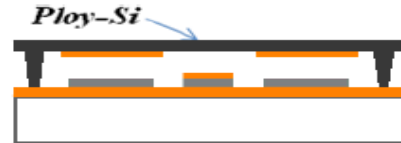

Fig. 14. Polysilicon deposition.

Fig. 15. Elimination of silicon oxide to release the switching electrode.

6. Conclusion

The proposed thermo-electrostatic actuated MEMS switch was simulated completely under quasi real conditions to investigate its proper dynamic operation and damping effects. Results showed improved and stable performance of the switch. All of the arms of the proposed switch were formed in the same surface and motion in the desired direction was guaranteed with respect to a bi-material additional system which was explained. This could not damage the switch because its temperature didn't increase so much and the silicon substrate underneath the arms wasn't destroyed.

So the mentioned problem for traditional switches was solved too. High frequency results showed good RF performance of the switch.

References

1. Rebeiz. G., *RF MEMS Theory, Design, and Technology*, John Wiley & Sons, Hoboken, NJ, 2003.

2. Nguyen. C. T. C., *RF MEMS for next generation wireless applications*, EECS, Michigan, 2000.

3. Rebeiz. G. M, Muldavin. J. B., *RF MEMS switches and switch circuits*, IEEE Microwave Mag., vol. 2, Dec. 2001, p. 59–71.

4. Muldavin. J. B, Rebeiz. G. M, *High-isolation CPW MEMS shunt switches—Part 1: Modeling*, IEEE Trans. Microwave Theory Tech., vol. 48, Jun. 2000, p. 1045–1052.

5. Muldavin. J. B, Rebeiz. G. M, *High-isolation CPW MEMS shunt switches—Part 2: Design*, IEEE Trans. Microwave Theory Tech, vol. 48, Jun. 2000, p. 1053–1056.

6. Persano. A, Tazolli. A, Cola. A, Sicliano. P, Meneghesso. G, Quaranta, F, *Reliability Enhancement by suitable Actuation Waveforms for Capacitive RF MEMS Switches in III-V Technology*, Journal of Microelectromechanical Systems, Vol. 21, Issue. 2, 2012, p. 414- 419.

7. Cho. J, Song. T, Baek. S and Yoon. E, *A Low-Voltage and Low Power RF MEMS Series and Shunt Switches Actuated by Combination of Electromagnetic and Electrostatic Forces*, IEEE Transactions on Microwave Theory and Techniques, Vol. 53, Issue. 7, Jul. 2005, p. 2450- 2457.

8. Girbau. D, Pradell. L, Lazaro. A, Nebot. A, *Electrothermally Actuated RF MEMS Switches Suspended on a Low-Resistivity Substrate*, Journal of Microelectromechanical Systems, Vol. 16, Issue. 5, Oct. 2007, p. 1061-1070.

9. Makasheva. K, Despax. B, Boudou. L, Teyssedre. G, *Dielectric Layers for RF MEMS Switches*, IEEE Transaction on Dielectrics and Electrical Insulation, Vol 19, Issue 4, 2012, p.1195- 1202.

10. Hennessy . R. P, Basu. A, Adams. A. A, McGruer. N. E, *Hot Switched Lifetime and Damage characteristics of MEMS Switch Contacts*, Journal of Micromechanics and Microengineering, Vol 23, 2013.

11. Kim J., Park J., Baek C., Kim Y., *The SiOG-Based Single-Crystalline Silicon (SCS) RF MEMS Switch with Uniform Characteristics*, Journal of Microelectromechanical Systems, Vol. 13, Issue. 6, 2004, p. 1036-1042.

12. Jr J. M., Ochoa H., Hinostroza V., *Design and Analysis of a MEMS Variable Capacitor Using Thermal Actuators, Journal of Computational Systems*, Vol. 10, Issue. 1, 2006, p. 1-15.

13. Muldavin. J. B., Rebeiz. G. M., *Nonlinear electro-mechanical modeling of MEMS switches*, in IEEE MTT-S Int. Dig., Phoenix, AZ, 2001, p. 2119–2122.

14. Bernstein. D., Guidotti. R., Pelesko. J.A., *Analytical and numerical analysis of electrostatically actuated MEMS devices*, in Proc. Modeling Simulation Microsyst, 2000, p. 489-492.

15. Gretillat. M. A., Yang. Y. J., Hung. E.S., V. R, abinovich. G.K. Ananthasuresh, N.F., de Rooij, Senturia. S.D., *Nonlinear electromechanical behavior of an electrostatic micro relay, in Transducers '97 IEEE Int. Conf. Solid-State Sensors and Actuators, Chicago, 1997, p.1141-1144.

16. Bernstein D., Guidotti R., Pelesko J.A., *Analytical and numerical analysis of electrostatically actuated MEMS devices*, in Proc. Modeling Simulation Microsyst., 2000, p. 489-492.

17. Shoji. Y, Kazuya. M, Kenichiro. S, *An Integrated Shunt Type MEMS Switch with a Submicron Narrow Gap*, Journal of Electronics and Communications in Japan, Vol. 95, Issue 11, 2012, p. 40- 48.

18. Nemirovsky Y., Bochobza-Degani O., *A methodology and model for the pull-in parameters of electrostatic actuators*, J. Microelectromech. Syst., Vol. 10, Issue. 4, 2012, p. 601- 615.

19. Siridejachai S., Ruttanapun C., Vannarat S., *Finite Element Model of Thermal Multimorph Actuator*, IEEE International Conference on Industrial Technology, Bangkok.

20. Peroulis. D, Pacheco. S. P, Sarabandi. K, Katehi L. P. B, *Electromechanical Considerations in Developing Low-Voltage RF MEMS Switches*, in IEEE TRANSACTIONS on Microwave Theory and Techniques. Vol. 51, Issue. 1, p. 259-269.